



## An effective design method for mechanical metamaterials with negative Poisson's ratios

---

Jie Xu, Hao Li, Mi Xiao and Liang Gao

EasyChair preprints are intended for rapid dissemination of research results and are integrated with the rest of EasyChair.

August 8, 2018

# An effective design method for mechanical metamaterials with negative Poisson's ratios

Jie Xu<sup>1</sup>, Hao Li<sup>1</sup>, Mi Xiao<sup>1</sup>, Liang Gao<sup>1\*</sup>

<sup>1</sup>*The State Key Laboratory of Digital Manufacturing Equipment and Technology, Huazhong University of Science and Technology, 1037 Luoyu Road, Wuhan, Hubei 430074, China*

Telephone number of the corresponding author: +86-27-87557742;

Fax of the corresponding author: +86-27-87559419

---

**Abstract:** In this paper, we propose a new method for the design of mechanical metamaterials by integrating the parametric level set method (PLSM) with the energy-based homogenization method (EBHM), where the topologies and shapes of material microstructures periodically distributed in the bulk material are optimized simultaneously. Firstly, material effective properties are evaluated by the EBHM under the topologies of material microstructures, where the average stress and strain theorems work as the basic theoretical framework rather than the asymptotic theory. Secondly, under the definition of the objective to seek for the negative Poisson's ratios, the PLSM is employed to evolve the topologies of microstructures until the bulk material is to be featured with negative Poisson's ratios. Several numerical examples for microstructures considering the orthotropy and isotropy are performed. A series of new and interesting material cells with negative Poisson's ratio are obtained.

**Keywords:** Metamaterials; Topology optimization; Parametric level set method; homogenization method.

## 1 Introduction

The structure of materials determines the properties and functions, while mechanical metamaterials establish the connection in material form and function. Due to the exotic properties, metamaterials are experiencing popularity in many emerging areas and engineering fields. It is noted that negative Poisson's ratio materials exhibit counter-intuitive properties: expanding laterally when stretched and contracting laterally when compressed [1]. However, only a limited number of natural materials [2,3] and artificial structures have been reported to exhibit negative Poisson's ratios.

Topology optimization has long been recognized as a powerful tool for the optimal design of both structures and materials [4], which iteratively eliminate and redistribute materials within a given design space to seek the best material layout. Until now, there are various approaches for the discipline of topology optimization, such as the homogenization method [5], the solid isotropic material with penalization (SIMP) [6], the evolutionary structural optimization (ESO) [7] and the level set method (LSM) [8], etc. Amongst them, a parametric level set method (PLSM) [9, 10] has been considered as a powerful level-set structural design method, which not only inherits the positive merits, but also eliminates the unfavorable features of the standard LSM. In the PLSM, the initial time-space coupled level set function is interpolated by the CSRBFs, so that the advancing of structural boundaries is equivalent to the evolution of the sizes of expansion coefficients of the CSRBFs. Moreover, many well-established efficient optimization algorithms can be directly applied into the PLSM to improve the optimization efficiency, e.g. the optimality criteria (OC) [11]. The PLSM has been applied to solve many problems.

Since the homogenization theory has been established, it is rapidly becoming popular to apply the topology optimization to seek the best layout for periodic RVE to enhance material properties [12, 13]. After the pioneering work of Sigmund who proposes an inverse design method by combing topology optimization with the numerical homogenization method [14]. The homogenization is used to evaluate the effective properties, and topology optimization is used to evolve the topologies of material cells until the expected effective properties is gained. Various materials with the novel mechanical or physical performances have been presented, such as extreme properties [15], maximum stiffness and fluid permeability [16], exotic thermomechanical properties [17] and negative Poisson's ratio [18]. Nevertheless, the majority of these existing methods are based on the material density-related interpolation schemes, which are featured with the conceptual simplicity and the numerical easiness but with several unexpected numerical features, like the numerical instability, intermediate density and zigzag boundary.

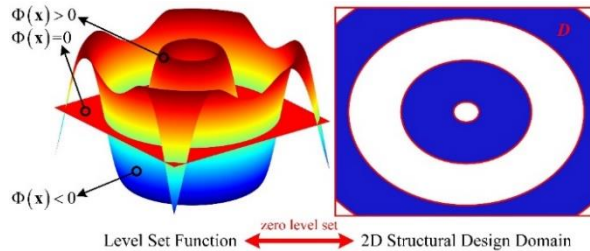
On the other hand, the numerical homogenization method (NHM) is utilized to evaluate material effective properties, which works as the bridge between the design of micro-structured materials and topology optimization [14]. It is well-known that the asymptotic expansion theory works as the basic framework of the NHM, while theoretical derivations and numerical implementations are relatively complex. As an alternative way, the energy-based homogenization method (EBHM) [20] has been proposed for the design of micro-structured materials, in which the average stress and strain theorems are the main theoretical basis to predict the materials effective properties. This paper will develop a new method for the design of mechanical metamaterials by integrating the PLSM with the EBHM, where the topologies and shapes of material microstructures periodically distributed in the bulk material are optimized simultaneously.

## 2 Parametric level set method

The main idea of the LSM lies in that the structural design boundary is implicitly described by zero level set of a higher dimension scalar function, as shown in **Fig. 1**. The different parts of a 2D design domain can be represent by the level set function, as follows:

$$\begin{cases} \Phi(\mathbf{x}) > 0, \forall \mathbf{x} \in \Omega \setminus \Gamma & (\text{material}) \\ \Phi(\mathbf{x}) = 0, \forall \mathbf{x} \in \Gamma \cap D & (\text{boundary}) \\ \Phi(\mathbf{x}) < 0, \forall \mathbf{x} \in D \setminus \Omega & (\text{void}) \end{cases} \quad (1)$$

Where  $\Omega$  is the structural design domain contained in reference domain  $D$ . The term  $\Gamma$  denotes the structural boundary at the zero level set.



**Fig. 1.** 3D LSF and the structural design domain

In the LSM, the dynamic evolution process of the structural boundary is formulated as the Hamilton-Jacobi partial differential function (H-J PDE) [8]. The merging and splitting of the design boundary towards its optimal can be mathematically governed by iteratively solving of the H-J PDE, written as:

$$\frac{\partial \Phi(\mathbf{x}, t)}{\partial t} - \mathbf{v}_n \cdot |\nabla \Phi(\mathbf{x}, t)| = 0 \quad (2)$$

where  $\mathbf{v}_n$  is the normal velocity field at the structural boundary.

It is summarized that structural topology optimization by using the LSM can be regarded as a dynamic evolution process of the level set surface via updating the normal velocity  $\mathbf{v}_n$ . However, as discussed previously, the direct solving of the H-J PDE to obtain the velocity field along boundary requires complicated numerical schemes [8]. In this article, the CSRBF with C2 continuity presented by Wendland [20] is adopted to parametrize the level set function. The LSF can be approximated by a series of CSRBFs and their expansion coefficients at different knots [9, 10].

$$\Phi(\mathbf{x}, t) = \boldsymbol{\varphi}(\mathbf{x})^T \boldsymbol{\alpha}(t) = \sum_{i=1}^N \phi_i(x) \alpha_i(t) \quad (3)$$

The LSF has been completely decoupled in Eq. (5), in which the CSRBF term  $\boldsymbol{\varphi}(\mathbf{x})$  is only spatial-dependent, while the expansion coefficient vector  $\boldsymbol{\alpha}$  is only time-dependent. For simplicity, the coordinates of CSRBF knots are assumed to be identical to the coordinates of FEA nodes.

Substituting Eq. (5) into Eq. (2), the H-J PDE can be rewritten as:

$$\boldsymbol{\varphi}(\mathbf{x})^T \frac{d\boldsymbol{\alpha}(t)}{dt} - \mathbf{v}_n \left| (\nabla \boldsymbol{\varphi}(\mathbf{x}))^T \boldsymbol{\alpha}(t) \right| = 0 \quad (4)$$

The normal velocity  $\mathbf{v}_n$  can be given by:

$$\mathbf{v}_n = \frac{\boldsymbol{\varphi}(\mathbf{x})^T}{\left| (\nabla \boldsymbol{\varphi}(\mathbf{x}))^T \boldsymbol{\alpha}(t) \right|} \cdot \frac{d\boldsymbol{\alpha}(t)}{dt} \quad (5)$$

Hereto, the standard LSM is transformed into a parametric form. It can be seen that  $\mathbf{v}_n$  is naturally extended to the whole design domain, and thus there is no need to employ additional schemes to extend the velocity field.

### 3 Energy-based homogenization method

In the scope of linear elasticity material, the local coordinate system  $\mathbf{Y}$  ( $\mathbf{Y}_{2d} = [0 Y_1] \times [0 Y_2]$ ) is utilized to define the RVE in the global coordinate system  $\mathbf{X}$ . The elastic property  $E^\zeta(\mathbf{x})$  is  $\mathbf{Y}$ -periodic function in the coordinate system  $\mathbf{X}$ . The parameter  $\xi$  denotes the scale of the RVE. The displacement field  $\mathbf{u}$  in the RVE can be characterized by a small asymptotic expansion equation. In this case, the homogenized elasticity tensor can be calculated in terms of material distributions.

$$E_{ijkl}^H = \frac{1}{|\mathbf{Y}|} \int_{\Omega} \left( \varepsilon_{pq}^{0(ij)} - \varepsilon_{pq}^{*(ij)} \right)^T E_{pqrs} \left( \varepsilon_{rs}^{0(kl)} - \varepsilon_{rs}^{*(kl)} \right) d\Omega \quad (i, j, k, l = 1, 2, \dots, d) \quad (6)$$

where  $|\mathbf{Y}|$  denotes the area in 2D or the volume in 3D of the RVE, and  $\varepsilon_{pq}^{0(ij)}$  is the initial unit strain. The strain field  $\varepsilon_{pq}^{*(ij)}$  of the RVE is obtained by solving the following linear elasticity equilibrium equation with  $\mathbf{Y}$ -period. In the EBHM, the initial unit test strain is directly imposed on the boundaries of PUCs. The induced strain field in PUCs corresponds to the superimposed strain fields  $\left( \varepsilon_{pq}^{0(ij)} - \varepsilon_{pq}^{*(ij)} \right)$  in Eq. (8), which is denoted by the symbol  $\varepsilon_{pq}^{Id(ij)}$ . Hence, Eq. (8) is transformed into a new form in terms of elementary mutual energies [17] by the induced displacement field in PUCs:

$$E_{ijkl}^H = \frac{1}{|\mathbf{Y}|} \sum_{e=1}^{NE} Q_{ijkl}^e = \frac{1}{|\mathbf{Y}|} \sum_{e=1}^{NE} \left( \mathbf{u}_e^{Id(ij)} \right)^T \mathbf{k}_e \mathbf{u}_e^{Id(kl)} \quad (7)$$

where  $\mathbf{u}_e^{Id}$  denotes the corresponding induced element displacements, and  $Q_{ijkl}^e$  stands for the elementary mutual energy. It is noted that the effective elasticity properties are interpreted as the summation of elastic energies of PUCs [15, 19].

### 4. Optimization design of mechanical metamaterials

In this paper, the latter one is investigated to gain materials with the Negative Poisson's ratio. The optimization model is established by integrating the PLSM with the EBHM:

$$\begin{aligned}
& \text{find : } \mathbf{\alpha}(\alpha_1, \alpha_2, \dots, \alpha_i, \dots, \alpha_N) \\
& \text{Maximize : } J = -E_{1212}^H + 0.03 \times (E_{1111}^H + E_{2222}^H) \\
& \text{subject to : } \begin{cases} V(\Phi) = \int_{\Omega} H(\Phi) d\Omega - V_{max} \leq 0 \\ a(\mathbf{u}^*, \mathbf{v}, \Phi) = l(\mathbf{v}, \Phi) \forall \mathbf{v} \in H_{per}(\Omega, \mathbf{R}^3) \\ \alpha^L \leq \alpha_i \leq \alpha^U \quad (i=1, 2, \dots, N) \end{cases}
\end{aligned} \tag{8}$$

where  $\mathbf{\alpha}$  denotes the vector of design variables,  $V$  is the volume fraction constraint with an upper bound of  $V_{max}$ .  $H$  is the Heaviside function.  $\alpha^L$  and  $\alpha^U$  are the lower and upper bound of the design variables, respectively. In the RVE, the linear elasticity equilibrium equation is stated in the weak variational form, in which the bilinear energy term  $a$  and the linear load form  $l$  can be written as:

$$\begin{cases} a(\mathbf{u}^*, \mathbf{v}, \Phi) = \int_D \varepsilon_{ij}(\mathbf{u}^*) E_{ijkl} \varepsilon_{kl}(\mathbf{v}) H(\Phi) d\Omega \\ l(\mathbf{v}, \Phi) = \int_D \varepsilon_{ij}(\mathbf{u}^0) E_{ijkl} \varepsilon_{kl}(\mathbf{v}) H(\Phi) d\Omega \end{cases} \tag{9}$$

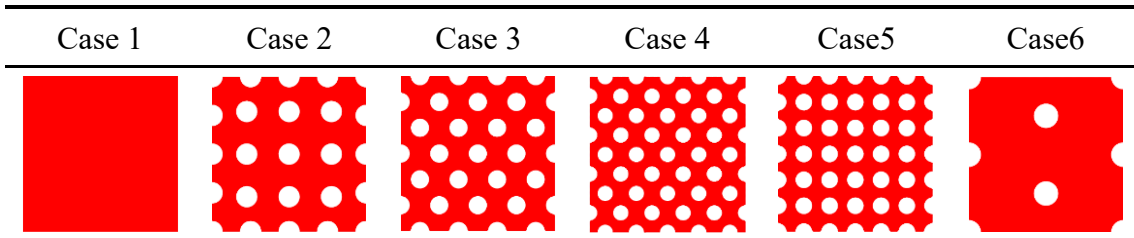
Moreover, the expansion coefficients, which are identified as the design variables, can be updated by the more efficient gradient-based optimization algorithms, rather than directly solving H-J PDE using the up-wind scheme. In the developed topology optimization formulation, the design analysis of the objective and constraint functions with respect to the design variables is used to derive their updating, and the final form is given:

$$\begin{cases} \frac{\partial E_{ijkl}^H}{\partial \mathbf{\alpha}} = \frac{1}{|\mathbf{Y}|} \int_D (\varepsilon_{pq}^{0(ij)} - \varepsilon_{pq}^{*(ij)})^T E_{pqrs} (\varepsilon_{rs}^{0(kl)} - \varepsilon_{rs}^{*(kl)}) \boldsymbol{\varphi}(\mathbf{x})^T \delta(\Phi) d\Omega \\ \frac{\partial V}{\partial \mathbf{\alpha}} = \frac{1}{|\mathbf{Y}|} \int_D \boldsymbol{\varphi}(\mathbf{x})^T \delta(\Phi) d\Omega \end{cases} \tag{10}$$

## 5 Numerical examples

In all examples, the Young's modulus for the solid material and the void phase are  $E_0^s = 1$  and  $E_0^v = 0.001$  respectively, and the Poisson's ratio is  $\mu = 0.3$ . The RVE has no definite sizes in actual. For numerical simplicity, the dimensionless of the RVE is defined as  $1 \times 1$ , which is discretized by a mesh of  $100 \times 100$ . The iteration will be terminated when the difference of the objective functions between two successive steps is less than  $10^{-4}$ . Six different initializations of the RVE are defined in Table 1, where the first three are uniformly distributed with some holes and the last is fully filled with materials. Hence, the optimization will be discussed in six cases in terms of initializations.

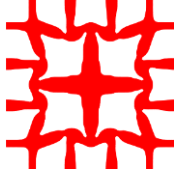
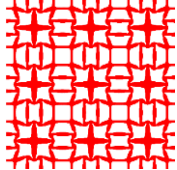
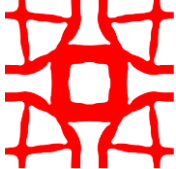
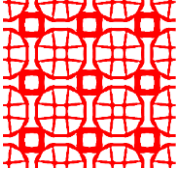





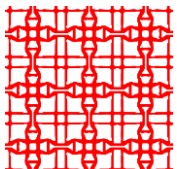


**Tab. 1 Six initializations of the RVE**



Six cases are still investigated to show the positive features of the proposed design method. In Tab. 2, The optimal results are provided including the defined volume fraction, the optimized RVEs with extreme shear modulus  $G$ , the  $3 \times 3$  Repetitive RVEs, the corresponding homogenized elastic tensor. It can be easily found that the periodical cellular materials with negative Poisson's ratio can be gained by the proposed design method, which further verify the validity. Similar to the above optimization designs, the optimized configurations of the RVE with negative Poisson's ratio are significantly

depended on the initializations. Compared with case 2 and 3 in the row 2 and 3 of Tab. 2, the optimized solutions are closer while the corresponding configurations are different. As far as the proposed method is concerned, there exists the nucleation mechanism of new holes within the design domain by analysing the case 4. Hence, the complex topological and shape evolution can be perfectly processed by deleting or generating holes as well as merging or splitting boundaries in the proposed design method. Moreover, the optimized topologies of the RVEs are all featured with smooth structural boundaries and distinct material interface due to the use of the PLSM, which shows the positive features of the developed design method again.

**Tab. 2** Optimal results with negative Poisson's ratio in six cases

Case	$V_{max}$	Optimized RVE	3×3 Repetitive RVEs	$E^H$	$\nu$
1	0.40			$\begin{bmatrix} 0.1232 & -0.0419 & 0 \\ -0.0419 & 0.1227 & 0 \\ 0 & 0 & 0.0064 \end{bmatrix}$	-0.34
2	0.40			$\begin{bmatrix} 0.1196 & -0.051 & 0 \\ -0.0511 & 0.1196 & 0 \\ 0 & 0 & 0.0074 \end{bmatrix}$	-0.43
3	0.40			$\begin{bmatrix} 0.1717 & -0.0508 & 0 \\ -0.0508 & 0.0590 & 0 \\ 0 & 0 & 0.0038 \end{bmatrix}$	-0.30
4	0.40			$\begin{bmatrix} 0.0910 & -0.0629 & 0 \\ -0.0629 & 0.1240 & 0 \\ 0 & 0 & 0.0038 \end{bmatrix}$	-0.76
5	0.40			$\begin{bmatrix} 0.1212 & -0.0525 & 0 \\ -0.0525 & 0.1212 & 0 \\ 0 & 0 & 0.0064 \end{bmatrix}$	-0.43
6	0.40			$\begin{bmatrix} 0.0477 & -0.0561 & 0 \\ -0.0561 & 0.1384 & 0 \\ 0 & 0 & 0.0052 \end{bmatrix}$	-1.18

## 6. Conclusions

This article proposes a new topological shape optimization method for the design mechanical metamaterials with negative Poisson's ratios. The design method systematically integrates the parametric level set method (PLSM) with the energy-based homogenization method (EBHM). In this method, the homogenized elastic properties of the RVE is evaluated by the EBHM, while the shape and topology changes of the RVE are evolved by the PLSM. From numerical examples, periodical cellular materials with negative Poisson's ratio are obtained.

## Acknowledgments

This work was supported by the National Basic Scientific Research Program of China [grant number JCKY2016110C012].

## References

- [1] Lakes R. *Science*, 1987, 235(4792):1038-1040.
- [2] B.D. Caddock, K.E. Evans, *J. Phys. D Appl. Phys.* 22 (1989) 1877–1882
- [3] A. Yeganeh-Haeri, D.J. Weidner, J.B. Parise, *Science* 257 (1992) 650–652.
- [4] O. Sigmund, K. Maute, *Struct. Multidiscip. Optim.* 48 (2013) 1031-1055.
- [5] M.P. Bendsøe, N. Kikuchi, *Comput. Meth. Appl. Mech. Eng.* 71 (1988) 197-224.
- [6] M. Zhou, G. Rozvany, *Comput. Meth. Appl. Mech. Eng.* 89 (1991) 309-336.
- [7] Y.M. Xie, G.P. Steven, *Comput. Struct.* 49 (1993) 885-896.
- [8] J.A. Sethian, A. Wiegmann, *J. Comput. Phys.* 163 (2000) 489-528.
- [9] Z. Luo, L.Y. Tong, Z. Kang, *Comput. Struct.* 87 (2009) 425-434.
- [10] Z. Luo, M.Y. Wang, S. Wang, P. Wei, *Int. J. Numer. Methods Eng.* 76 (2008) 1-26.
- [9] M.Y. Wang, X. Wang, D. Guo, *Comput. Meth. Appl. Mech. Eng.* 192 (2003) 227-246.
- [10] G. Allaire, F. Jouve, A.-M. Toader, *J. Comput. Phys.* 194 (2004) 363-393.
- [11] G. Rozvany, M. Bendsøe, U. Kirsch, *Appl. Mech. Rev.* 49 (1996) 54-54.
- [12] O. Sigmund, *Int. J. Solids Struct.* 31 (1994) 2313-2329.
- [13] O. Sigmund, S. Torquato, *J. Mech. Phys. Solids.* 45 (1997) 1037-1067.
- [14] B. Hassani, E. Hinton, *Comput. Struct.* 69 (1998) 707-717.
- [15] Gao J, Li H, Gao L, et al. *Adv. Eng. Softw.* 116 (2018) 89-102.
- [16] V.J. Challis, J.K. Guest, J.F. Grotowski, A.P. Roberts, *Int. J. Solids Struct.* 49 (2012) 3397-3408.
- [17] Y. Wang, J. Gao, Z. Luo, T. Brown, N. Zhang, *Eng. Optimiz.* 49 (2017) 22-42.
- [18] O. Sigmund, *Mech. Mater.* 20 (1995) 351-368.
- [19] L. Xia, P. Breitkopf, *Struct. Multidiscip. Optim.* 52 (2015) 1229-1241.
- [20] H. Wendland, *Adv. Comput. Math.* 4 (1995) 389-396.